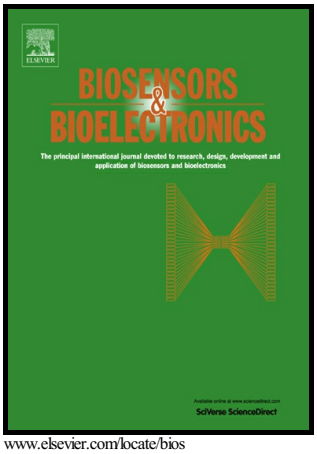

www.elsevier.com/locate/bios

Ultrasensitive nanostructure sensor arrays on flexible substrates for multiplexed and simultaneous electrochemical detection of a panel of cardiac biomarkers

Nandhinee Radha Shanmugam, Sriram Muthukumar, Shajee Chaudhry, Jonathan Anguiano, Shalini Prasad

PII: S0956-5663(16)31066-1
DOI: http://dx.doi.org/10.1016/j.bios.2016.10.046
Reference: BIOS9268

To appear in: *Biosensors and Bioelectronic*

Received date: 11 July 2016
Revised date: 17 October 2016
Accepted date: 19 October 2016

Cite this article as: Nandhinee Radha Shanmugam, Sriram Muthukumar, Shaje Chaudhry, Jonathan Anguiano and Shalini Prasad, Ultrasensitive nanostructure sensor arrays on flexible substrates for multiplexed and simultaneou electrochemical detection of a panel of cardiac biomarkers, *Biosensors an Bioelectronic,* http://dx.doi.org/10.1016/j.bios.2016.10.046

Biosensors and Bioelectronics

Ultrasensitive nanostructure sensor arrays on flexible substrates for multiplexed and simultaneous electrochemical detection of a panel of cardiac biomarkers

Nandhinee Radha Shanmugam[a], Sriram Muthukumar[b], Shajee Chaudhry[c], Jonathan Anguiano[a], Shalini Prasad[a*]

[a]*Department of Bioengineering, University of Texas at Dallas, 800 West Campbell Road, Richardson, TX 75080, USA*
[b]*Enlisense LLC, 1813 Audubon Pond way, Allen, TX 75013, USA*
[c]*Department of Natural Sciences & Mathematics, University of Texas at Dallas, 800 West Campbell Road, Richardson, TX 75080, USA*
*Corresponding author: *E-mail address:* shalini.prasad@utdallas.edu

Abstract

Multiplexed detection of protein biomarkers offers new opportunities for early diagnosis and efficient treatment of complex diseases. Cardiovascular diseases (CVDs) has the highest mortality risk in USA and Europe with 15-20 million cases being reported annually. Cardiac Troponins (T and I) are well established protein biomarkers associated with heart muscle damage and point-of-care monitoring of both these two biomarkers has significant benefits on patient care. A flexible disposable electrochemical biosensor device comprising of vertically oriented zinc oxide (ZnO) nanostructures was developed for rapid and simultaneous screening of cardiac Troponin-I (cTnI) and cardiac- Troponin-T (cTnT) in a point-of-care sensor format. The biosensors were designed by selective hydrothermal growth of ZnO nanostructures onto the working electrodes of polyimide printed circuit board platforms, resulting in the generation of high density nanostructure ZnO arrays based electrodes. The size, density and surface terminations of the nanostructures were leveraged towards achieving surface confinement of the target cTnT and cTnI molecules on to the electrode surface. Multiplexing and simultaneous detection was achieved through sensor platform design comprising of arrays of Troponin functionalized ZnO nanostructure electrodes. The sensitivity and specificity of the biosensor was characterized using two types of electrochemical techniques; electrochemical impedance spectroscopy (EIS) and Mott-Schottky analysis on the same sensor platform to demonstrate multi-configurable modes. Limit of detection of 1 pg/mL in human serum was achieved for both cTnI and cTnT. Cross reactivity analysis showed the selectivity of detecting cTnT and cTnI in human serum with wide dynamic range.

Keywords: Multiplexed detection, cardiac Troponins, ZnO nanostructures arrays, EIS, Mott-Schottky, point-of-care

1. Introduction

Early detection and reliable diagnosis play a central role in making effective therapeutic decisions for treatment of diseases. Detection involves identification of disease-specific biomarkers (i.e. proteins, DNA or RNA, metabolites, etc.) in human body fluids (i.e. blood, plasma, urine, etc.) that represents the irregularities in cellular regulatory functions, pathological responses or intervention to any therapeutic drugs (Neumann 2015). Quantitative detection of these biomarkers in a simultaneous or multiplexed manner at the early stages of the disease when expressed in very low concentrations has been a technological challenge. Also, accuracy in diagnosis is further enhanced when the quantification of the disease can be done through a panel of biomarkers (Joos et al. 2002). Hence there is immense interest and value in designing ultrasensitive biosensors towards detection of a panel of biomarkers from a single sample of human body fluids.

A number of transduction strategies have been adopted to achieve the goal of ultra-sensitive and multiplexed label-free detection. One leading methodology that is widely implemented by

electrical/electrochemical based biosensor platforms relies on detecting and capturing the biomarkers on the surface of electrode materials which transduces the biological signal in to a measurable electrical signal response (Agah et al. 2005; Daniels and Pourmand 2007). The structural and morphological characteristics of the electrode materials thus play a key role in achieving both sensitivity and selectivity required for ultrasensitive biomarker detection (North et al. 2010). At nanoscale, precise control over size and shape yield nanostructures with enhanced chemical and physical properties that can be tailored towards designing robust biosensor platforms (Feigel et al. 2011). Moreover, the availability of large number of surface atoms in the nanostructures allows for amplification of biological signal response when compared to its planar counterparts thus enabling improved sensing characteristics.

Recently, synthesis and characterization of ZnO for wide range of applications have triggered more research interest due to its multifunctional and nano-morphological characteristics. Properties like high isoelectric point and high catalytic efficiency have been leveraged extensively towards design of ZnO nanostructure based enzymatic biosensors for detection of glucose, cholesterol, lactic acid, uric acid, etc. (Lei et al. 2012; Liu et al. 2013; Marie et al. 2015; Wang et al. 2006). However, quantification of above mentioned analytes is based on detection of byproducts of those enzymatic reactions whereby non-specific interactions becomes an issue. Technological bottlenecks associated with non-specific interactions can be minimized by use of specific capture probes (Joos et al. 2002). Affinity based sensing mechanisms for designing immunoassay based biosensors using non-faradic approach have been investigated widely but implementation on ZnO as a sensing material has been relatively limited. As a direct and wide bandgap semiconducting material, ZnO nanostructures facilitate direct electron transport as their electrical properties are strongly altered by the charge perturbations occurring due to biomolecular confinement and binding events (Hewlett and McLachlan 2016; Koval and Howard 1992). In this paper, we have focused our efforts in designing an ultrasensitive biosensor platform for multiplexed detection of protein biomarkers based on ZnO nanostructures.

The electrical detection methodology provides the means to directly characterize the capture probe – target biomarker interactions based on charge perturbations at the electrode / electrolyte interface (Bard et al. 1993). When ZnO electrode is treated with ionic solution consisting of biomolecules, a potential difference is created at the electrode/electrolyte interface due to the unequal distribution of charges. As a consequence of biomolecular binding events at ZnO nanostructure surface, redistribution of charges in the electrode and ions in the electrolyte result in formation of space-charge region within ZnO and electrical double layer at the interface (Morrison 1980). Evaluation and quantification of biomarker binding can thus be achieved by measuring the changes in electrode resistance or capacitance at selected frequencies. In our previous work, we have characterized the changes to space-charge capacitance and overall impedance at ZnO nanoelectrode/electrolyte interfaces using both Mott-Schottky technique and electrochemical impedance spectroscopy (EIS) respectively towards detection of cardiac Troponin-T (Shanmugam et al. 2016). Correlation in output signal response with concentration was established between both the detection techniques and hence can be used as combinatorial approaches for accurate and sensitive detection of protein biomarkers. However, identifying disease heterogeneity using an individual protein biomarker alone is inadequate. Though this studies show sensitive detection of single biomarker, often simultaneous detection of multiple biomarkers is recommended for accurate clinical diagnosis.

The availability of wide panel of biomarkers associated with a disease which if detected and quantified, can not only provide clinical intervention to state of a disease but also increase the survival rate of patients suffering from cancer and cardiovascular diseases (CVD) (Qureshi et al. 2012). Patients presenting to emergency rooms complaining of chest pain often experience unpredicted cardiac events and are mostly discharged with non-cardiac diagnoses only to experience a heart attack later (Thygesen et al. 2012). Myocardial infarction (MI) which accounts for nearly 1.5 million deaths annually occurs when myocardial

cellular functions are affected due to reduced blood supply exceeding the critical threshold limit. Qureshi et al. discusses the availability of several biomarkers representing different stages of CVD and range of biosensors developed for its detection (Qureshi et al. 2012). Cardiac Troponin-I (cTnI) and Troponin-T (cTnT) have been established as highly specific and sensitive gold standard biomarkers for myocardial cell death and its subsequent events (Ahmad and Sharma 2012; Jaffe et al. 2006). Early studies with cTnI and cTnT has elucidated these markers for detection of MI with recommendation of 99^{th} percentile reference limits (Apple 2001; Apple et al. 2005). Though existing technologies and developments in bioassays have shown great potential for disease diagnosis, its dependencies such as infrastructure, sample preparation and turnaround time makes it challenging (McDonnell et al. 2009). To overcome these limitations, the key is to design and develop a biosensor platform suitable for use in a resource limited settings capable of analyzing proteomic profiles of multiple cardiac protein biomarkers in a complex biological sample. The diagnostic breakthrough in MI diagnosis was the development and commercialization of devices capable of monitoring cardiac Troponins (Roche Cobas h232, Abbott i-STAT, etc.) (Apple 2001). The gap in these devices is the multiple single analyte tests and cost of detection that significantly adds cost burden to patients. Hence, there is demand and challenges to develop an ultrasensitive biosensor platform for multiple biomarker detection from low sample volume.

Multiplexed immunoassays have recently garnered interest due to their ability to detect multiple analytes simultaneously in short period of time from a small sample volume and reduced cost (Joos et al. 2002). Taking advantage of its nanoscale dimensions and simplicity of detection methods (Balasubramanian 2010), arrays of ZnO nanostructures can be integrated with microelectrode platforms to design miniaturized and portable electrical nanobiosensor devices for point of care applications. In this work, we describe the design and development of zinc oxide (ZnO) nanostructured sensing platform on flexible polyimide substrates leveraging the affinity interactions between the antibody and antigen, coupled with EIS and/or Mott-Schottky for accurate detection of multiple biomarkers, cTnI and cTnT in human serum. Though our previous study demonstrates the ability of nanostructured ZnO platform to sensitively detect cTnT with lower limit of detection at 0.1 pg/mL, we significantly extend and enhance the capabilities of this platform for simultaneous detection of cTnI and cTnT. The antibodies (α-cTnT and α-cTnI) were selectively immobilized on ZnO decorated electrode arrays. The interaction of target biomarkers (cTnI and cTnT) with its antibody led to changes in direct electrochemical responses i.e. change in space charge capacitance (C_{sc}) and impedance due to increase in spatial blocking that alters the electrical performance of ZnO nanostructures. The specificity and cross-reactivity of these antibodies is also established. We observe the limit of detection at 1 pg/mL for both cTnI and cTnT. These preliminary studies show great promise for future development of this platform for multiplexed and simultaneous detection of cTnI and cTnT with good analytical performance in real-time.

2. Materials and Methods

2.1. Materials and reagents

The precursors for hydrothermal growth – zinc nitrate hexahydrate (Zn(NO3)2 .6H2O) and hexamethylenetetramine (HMTA) with 99.5% purity and reagent grade were procured from Acros Organics (Fisher Scientific, MA, USA). The amine reactive crosslinker molecule – (dithiobis(succinimidyl propionate)) (DSP; Pierce Biotechnologies) and its solvent dimethyl sulfoxide (DMSO) were purchased from Thermo Fisher Scientific (MA, USA). The monoclonal antibodies and recombinant protein stock aliquots for cTnI and cTnT were obtained from US Biological Life Sciences (MA, USA) and Abcam (MA, USA) respectively. Phosphate buffered saline (PBS) for preparing aliquots of antibody and antigen and bovine serum albumin

(BSA) for cross reactivity studies were purchased from Sigma Aldrich (MO, USA). Human Serum (HS) for preparing dilutions of cardiac biomarkers was purchased from Fisher Scientific (MA, USA).

2.2. Multiplexed sensor array design, assembly and measurements

The sensor array for multiplexed detection was designed based on three-electrode electrochemical setup, which was all prepared in flexible polyimide using standard thin film fabrication technologies. A few nm of ZnO seed layer was selectively deposited on the working electrodes using RF-Magnetron sputtering technique. ZnO seed layer acts as the nucleation sites for growth of ZnO nanostructures when subjected to low temperature hydrothermal bath consisting of $Zn(NO_3)_2.6H_2O$ and HMTA dissolved in deionized water. The hydrothermal growth parameters have been optimized and established in our previous work (Shanmugam et al. 2016). Following the hydrothermal growth, the sensor substrates are washed with deionized water and dried under nitrogen to prepare the sensor for assembly. A microfluidic encapsulant was prepared using polydimethylsiloxane (PDMS), an elastomeric polymer to hold the sample volume less than 50 µL. PDMS encapsulant were bound to sensor substrates using water resistant adhesive. The electrical connections with the electrochemical instrumentation were established at the connector pads. In EIS, a small amplitude sinusoidal voltage of 10 mV peak-to-peak over the wide frequency range of 0.1 Hz to 1 MHz was applied and resulting response was measured as impedance of the system. The Mott-Schottky capacitance ($1/C^2$) is measured as function of applied DC potential (-1 V to +1 V) at fixed frequency. These electrochemical measurements were taken using Gamry Reference 600 potentiostat (Gamry Instruments, PA). A schematic representation of multiplexed sensor with block diagram of system interface is shown in Fig.1.

2.3. ATR-FTIR spectroscopy

Attenuated Total Reflectance Fourier Transform Infrared (ATR-FTIR) spectroscopy of surface functionalized ZnO nanostructures were obtained using Nicolet 6700 FTIR spectrometer equipped with a deuterated, L-alanine doped triglycine sulfate (DLaTGS) detector with KBr Window and Validation Motor. The spectrometer was fitted with a sampling stage (ValPro Qualified Smart Orbit for Nicolet X700) equipped with a 60° diamond ATR crystal and the sample was held with a swivel clamp that applied an even and constant force during the acquisition of the spectra. Each FT-IR spectrum collected on the sample represents the average of 200 scans at 4 cm^{-1} resolution in the scan range of 4000 – 400 cm^{-1}.

Samples for FTIR analysis were prepared as follows. A thin layer of gold were deposited on the glass slides followed by ZnO seed deposition. The glass slides were cleaned subsequently in acetone, isopropyl alcohol and deionized water prior to use. The nanostructures of ZnO were grown on seeded substrates and washed with DI water to remove growth residues. The nanostructured ZnO substrates were then treated with 10 mM DSP in DMSO for an hour. After DSP functionalization, the substrates were rinsed with DMSO to remove unbound molecules and stored with silica desiccants for analysis. Some of the samples were washed with PBS immediately and then treated with α-cTnI antibody. After 30 minutes, the antibody treated substrates were washed with PBS and analysis was performed.

2.4. Preparation of Immunoassay

The nanostructures of ZnO were functionalized by formulating 10 mM DSP in DMSO and allowing the sample to interact with the sensor substrate for an hour. The NHS ester group at its terminal end provides amino-reactive surface that forms amine linkage with primary amine groups in the antibody molecule. The monoclonal antibodies, α-cTnT and α-cTnI are selectively immobilized on the working electrodes at 1 µg/mL

concentration in PBS for 30 minutes at room temperature. Following antibody immobilization, the unbound DSP sites are blocked with Superblock to eliminate non-specific binding interactions. The serial dilutions of both the antigens (cTnI and cTnT) for calibration experiments were prepared in HS with varying concentrations – 0.1 pg/mL, 1 pg/mL, 10 pg/mL, 100 pg/mL, 1E4 pg/mL 1E5 pg/mL and 1E6 pg/mL. The antigen aliquots spiked in HS were then tested on the sensor arrays starting with the lowest concentration and incubation time of 15 minutes. Several wash steps (3x) were performed using corresponding buffers (DMSO / PBS / HS) in between each step to remove the excess of any unbound molecules. The immunoassay for both cTnI and cTnT detection with ZnO nanostructures as sensing surface are illustrated in Fig.1. A total of n=3 replicates were performed for each experimental design.

3. Results and Discussion

The multiplexed sensor array in this paper consists of two arrays (array 1 and array 2) as shown in Fig.1, with ZnO nanostructures selectively grown on working electrodes (WE) and are used for electrochemical detection of different isoforms of cardiac biomarkers, cTnI and cTnT. Baseline electrical characterization of this sensor design was experimentally verified using electrochemical impedance response at 100 Hz. Detection of cTnI and cTnT was demonstrated using EIS and Mott-Schottky techniques.

3.1. Characterization of functionalized and antibody immobilized ZnO nanostructures

ZnO nanostructures of aspect ratio ~4 were selectively grown on the working electrodes using low temperature aqueous hydrothermal growth mechanism. Fig.2(A) shows the SEM micrograph of ZnO nanostructures grown by tuning the chemical reactions between the precursors $Zn(NO_3)_2.6H_2O$ and HMTA dissolved in water. The thermal decomposition and hydrolysis reactions of these precursors results in the formation of zinc hydroxyl species which upon dehydration form ZnO nuclei. The pre-seeded regions in the sensor design now acts as the nucleation sites for the aligned growth of ZnO nanostructures. The higher surface energy difference between polar and non-polar planes drives faster growth of ZnO along polar planes resulting in c-axis oriented crystalline growth of wurtzite ZnO nanostructures. SEM imaging confirmed the morphology of synthesized ZnO nanostructures as vertically grown hexagonal shaped rod-like structures and uniform growth on both the multiplexed sensor arrays. The morphology of ZnO nanostructures is shown with AFM scan image in Fig 2(B). Both SEM and AFM characterization demonstrates clearly the uniform growth of hexagonal shaped ZnO nanostructures at pre-seeded working electrodes of multiplexed sensor array. The as-synthesized nanostructures were used to demonstrate detection of target cardiac biomarkers following the immunoassay protocol as detailed in experimental section.

ATR-FTIR spectra of DSP modified and antibody immobilized ZnO nanostructured sensing surface are shown in Fig.2(C) in the range between 2000 cm^{-1} and 500 cm^{-1}. The results in Fig.2(C) show the spectra (top spectra) for the functionalization of ZnO nanostructures with thiol based DSP linker molecules, which provide binding sites for antibody immobilization. The peak at 571 cm^{-1} is associated with ZnO nanostructure arrays and is stable during all the immunoassay steps. The peaks observed at 1053 cm^{-1} and 1314 cm^{-1} are assigned to stretching vibrations of ν(C-O) and ν(N-O) respectively. The spectral features ν(C-O) is characteristic of the ester linkage and ν(N-O) represents the symmetric stretch of nitro groups both of which disappears with immobilization of antibody molecule. The other succinimidyl identifier groups that show evidence of DSP binding to ZnO surfaces are the carbonyl stretch in primary amides (ν(C=O)) at 1662 cm^{-1} and bending vibrations of alkane stretch (ν(C-H)) with two peaks at 2915 cm^{-1} and 3000 cm^{-1} (not shown). Bands assigned at 1411 cm^{-1} and 1436 cm^{-1} are characteristic of methylene scissors deformation in the bound DSP molecule. Appearance of broad band between 1200 cm^{-1} and 1020 cm^{-1} in Fig.2(C) bottom spectra is characteristic of

ν(C-C, C-N) confirms aminolysis of NHS groups in DSP with primary amines in antibody establishing a stable conjugation of the antibody to the linker functionalized ZnO nanostructure surfaces grown on Au electrodes.

3.2. COMSOL simulation of multiplexed sensor array

The use of finite element approach to simulate the real time behavior was used to virtually understand the performance thereby aiding in optimizing the multiplexed sensor array design to meet the desired characteristics which reduces the fabrication cost and time. We present the finite element model of our sensor substrate using the finite element software, COMSOL Multiphysics, to establish that the arrays of multiplexed sensor offer same baseline electrical performance.

The model encompasses the electrode geometry constructed in three dimensional space and simulations performed using AC/DC module with assumption of no magnetic field effects. Fig.3(A) shows an illustration of 2D schematic of geometric model (similar to schematic in Fig.1) in COMSOL domain with applied boundary conditions. The geometric structures consisted of three microelectrodes built on polyimide substrate and surrounded by a rectangle made of PBS. Electrical properties of gold were assigned to both the CEs and a RE whereas WEs were assigned the properties of ZnO. A constant applied potential of 10 mV was set at the WE. The boundary condition of both the RE and the CE was set at zero potential. Electrical insulation with a von Neumann boundary condition (n.J = 0) was applied to the PBS layer. The transient electric field is assumed to be confined within the multiplexed electrodes and the surrounding PBS medium and is governed by the following continuity equation.

$$\nabla . J = Q_j \quad i.e.\ \nabla . \sigma E = -\frac{\partial \rho}{\partial t}$$

where σ is the electrical conductivity, ρ is the charge density. Based on Ohm's law, a relation between the current density, J (vector quantity) and the electric potential, V (scalar quantity) can be established. The electric field E, can be obtained from the following constitutive relation and the gradient of the scalar potential V as shown.

$$D = \varepsilon_o \varepsilon_r E$$
$$E = -\nabla V$$

In above equations, D is the displacement current, ε_o is the permittivity of free space and ε_r is the relative permittivity of the material/electrolyte used. The discretization of the designed system into finite elements were based on physics controlled mesh generation.

Fig.3 shows the current distribution in the multiplexed sensor array for simulations performed with earlier described boundary conditions. Surface plot in Fig.3(B) shows uniform distribution of current density between three electrodes in both the array formats. We observe maximum current density near the surface of WEs which indicates that the output current response measured in EIS is from the WE. The graph illustrates the variation in current density with distance between WE and CE in Fig.3(C) and between WE and RE in Fig.3(D) measured along the dotted lines represented in Fig. 3(A). The results indicate that both WEs exhibit same performance along its surface and in three electrode setup. Farther the measured points away from the WE, current density decreases with highest value of 1.7 x 10^{15} A/m^2 observed at its surface. In addition, the direction of arrows in Fig.3(B) corroborates that the electric field lines are directed away from positive surface and performed simulations are correct. These results confirm that both WEs exhibit same baseline electrical performance under ideal conditions and thus placement of electrodes in multiplexed sensor array have minimal to no variation. Surface modification of electrode arrays perturbs the charge distribution at the electrode/electrolyte interface. These perturbations are based on realignment of electrons or holes in the

electrode surface and ions in the electrolyte solution. Thus, these charge perturbations can be leveraged towards designing biosensors for multiplexed detection of cardiac biomarkers.

3.3. Baseline electrical characterization of multiplexed sensor array

The baseline electrochemical response of the multiplexed sensor arrays was characterized in presence of supporting electrolyte – PBS at 10 mV peak-to-peak at 100 Hz. The open circuit (OC) potential at both array 1 and array 2 was measured to establish that the same electric potential exists on both the sensor arrays. It is the potential experienced at the working electrode relative to reference electrode before any electrochemical reaction occurs and was estimated at 0.02 V i.e. 25.0 ± 1.8 mV in array 1 and 24.6 ± 1.6 mV in array 2. Similarly, the short circuit (SC) potential was measured in presence of PBS and was observed at 0.01 V i.e.18.2 ± 0.8 mV in array 1 and 17.2 ± 0.5 mV in array 2. The impedance response at each step of immunoassay (described in experimental section) was characterized for both the arrays as shown in Fig. 4. Upon functionalization of ZnO surfaces with DSP, the thiol functional group in DSP binds to the Zn sites in the nanostructures forming Zn-S bond. The charged electrodes in presence of an ionic buffer medium experience alignment of charges at the electrode surface forming electrical double layer (EDL). A modified Randles equivalent circuit was used to study the contribution due to capacitive and resistive elements. The charge conduction between the electrode and the ionic buffer constitute the charge transfer resistance (R_{ct}) and resistance offered by the buffer constitute the solution resistance (R_s) in the electrochemical signal response. This amine reactive 8-carbon spacer molecule in DMSO is highly resistive and hence higher impedance response was obtained. The impedance for DSP step increased from baseline impedance of 2.9 kΩ to 1792 kΩ and 2.7 kΩ to 1701 kΩ in array 1 and array 2 respectively. The difference in impedance between the sensor arrays can be attributed to density of functionalization and is within the acceptable coefficient of variation for electrical biosensors (CV<10%). Following the functionalization protocol, the ZnO nanobiosensor arrays were prepared for antibody immobilization by performing 3x wash with DMSO followed by 3x PBS wash. The decrease in impedance observed with PBS wash post functionalization is due to the conducting molecules that is present in the buffer. For these characterization studies, cTnT was used to establish consistency in electrical performance between array 1 and array 2 during the immunoassay steps. When antibody (α-cTnT) is immobilized the charges in the outer plane realign and this arrangement is analogous to that of a parallel plate capacitor that constitute double layer capacitance (C_{dl}). The impedance response at array 1 and array 2 decreased to 9.1 kΩ and 8.1 kΩ respectively due to binding of α-cTnT to linker molecule. Post wash step with PBS, the multiplexed sensor arrays were treated with a blocking buffer to block any unbound DSP sites and measured impedance was 8.1 kΩ and 7.5 kΩ respectively at array 1 and array 2. The order of testing the arrays did not affect the impedance responses of the multiplexed sensor array. The sensor arrays were then washed with PBS to prepare them for performing antigen dose response studies. The noise in the system is estimated as change in output signal response between pre- and post- buffer wash after superblock step. The recommendation for signal noise threshold for any electrical biosensor is 3 times the noise and noise estimation for both the detection techniques is given in next section.

3.4. Multiplexed and simultaneous detection of cTnI and cTnT in HS buffer

Immunoassays for cTnI detection was performed at array 1 and that for cTnT detection was performed at array 2 as shown in Fig. 1, for establishing the multiplexed and simultaneous detection of sensor performance. Sensor array preparation for detection of these cardiac biomarkers consisted of immunoassay steps explained in previous section. Thus prepared sensor is first tested with neat HS which consists of zero concentration of measured protein biomarker to establish zero dose measurement. It is used to characterize signal change as

function of antigen binding to antibody immobilized surfaces. Different concentrations of cTnI antigen starting with the lowest concentration were tested on α-cTnI immobilized ZnO nanostructure surface at array 1. Similarly, different doses of cTnT antigen were tested on α-cTnT immobilized ZnO nanostructure surface at array 2. The change in output signal response for subsequent doses is calculated from zero dose measurement to obtain a calibration curve for cTnI and cTnT detection. In this work, percentage change in measured signal was chosen to represent the multiplexed sensor performance. Detection of cTnI and cTnT was demonstrated using both EIS and Mott-Schottky techniques.

3.4.1. Detection using EIS

The detection of cTnI and cTnT with multiplexed sensor arrays using EIS is represented as Nyquist plots in Fig. 5(A) and Fig. 5(B) and as calibration curves in Fig. 5(C) and Fig. 5(D) respectively. A decrease in capacitive impedance is observed with increasing concentration of tested protein biomarker as shown in Nyquist plots in Fig. 5(A) and Fig. 5(B). Analysis of corresponding Bode phase plots revealed the lag in output signal response (59˚ for cTnI detection and 62˚for cTnT detection) which corroborates the maximum contribution to output signal response is dominated by capacitance at the double layer, C_{dl}. With increasing concentrations of tested biomarker binding to antibody immobilized ZnO surfaces, the charge distribution at EDL is perturbed resulting in a dominating capacitive impedance observed at 100 Hz. Fig. 5(C) and Fig. 5(D) shows respectively the linear response of detection for cTnI and cTnT across the tested concentration ranges 0.1 pg/mL to 1E5 pg/mL. We observed a dynamic change of 58 % for cTnI detection resulting from impedance range between 4.7 kΩ and 1.9 kΩ. Similarly, the range of impedance observed for cTnT detection was between 5.8 kΩ and 2.2 kΩ that resulted in dynamic range of 61% for cTnT detection. The signal noise threshold was calculated as three times the change in impedance response between pre- and post- buffer wash post blocking step in immunoassay. The observed signal noise threshold for cTnI detection at array 1 was 8.8% and for cTnT detection at array 2 was 7.4%. The lowest concentration that can reliably be detected using multiplexed sensor arrays was evaluated to be 1 pg/mL for cTnI and 0.1 pg/mL for cTnT detection.

3.4.2. Detection using Mott-Schottky

Fig. 6(A) and Fig. 6(B) shows the Mott-Schottky capacitance ($1/C^2$) plotted as a function of applied potential for cTnI and cTnT detection using nanostructured ZnO multiplexed sensor arrays. Mott-Schottky plots were obtained with a voltage sweep of -1 V to +1V and input signal amplitude of 10 mV peak-to-peak at 1000 Hz. A smaller change in capacitance ($1/C^2$) with increasing concentrations of tested doses of cardiac biomarker was obtained. Fig. 6(A) shows linear increase in $1/C^2$ at potentials higher than 0.3 V for cTnI detection which is as expected for an n-type ZnO. At applied potential higher than 0.7 V, the response $1/C^2$ reached its limiting value and hence 0.7 V was chosen to represent change in $1/C^2$ with cTnI antigen binding. Similar response was observed for cTnT detection in Fig. 6(B). The range of $1/C^2$ obtained was between 144.8 and 86.4 $(1/\mu F)^2$ for cTnI whereas for cTnT detection, $1/C^2$ values obtained was in the lower range from 76.12 to 26.38 $(1/\mu F)^2$ with increasing concentrations of tested dose. This trend is consistent with the response obtained with EIS. Absolute values are shown in supplementary in Fig. S2. The calibration curve is built to represent the percentage change in Mott-Schottky capacitance with varying concentrations. Fig. 6(C) shows the calibration curve for cTnI with 47 % dynamic change in output response. The signal noise threshold was estimated at 11.5 % and hence the reliably detected lowest concentration of cTnI with MS is 1 pg/mL. Similarly, the calibration curve for cTnT detection is shown in Fig. 6(D). The dynamic change of 67% was obtained with detectable lowest cTnT concentration at 1 pg/mL. The estimated noise threshold for cTnT array was 9.2 %. We attribute the slightly higher signal noise threshold on Mott-Schottky capacitances relative to

that of EIS plots to be due to the microelectrode layout. Analysis of Mott-Schottky plots yielded donor densities of 10^{22} cm^{-3} for the semiconducting ZnO nanostructures which is consistent with our previously published results.

3.5. Evaluation of non-specificity and cross-reactivity

A sensor performance is termed reliable only when it can specifically detect the target isoform of protein biomarkers in the presence of other similar protein biomarkers. In this preliminary study, the non-specificity of α-cTnT for cTnI isoform and α-cTnI for cTnT isoform were tested over the range of concentrations between 0.1 pg/mL and 1E5 pg/mL. The electrochemical signal response in Fig. 5(C-D) and Fig. 6(C-D) indicates that only the corresponding target isoform shows a decrease in capacitive impedance (i.e. increase in percentage change in EIS impedance and Mott-Schottky capacitance) with increasing dose concentration, while the signal response due to the non-specific isoform is well within the established signal noise threshold. The non-specificity of α-cTnI and α-cTnT for alternating isoforms with EIS is shown in Fig. 5(C) and Fig. 5(D) respectively and with Mott-Schottky in Fig. 6(C) and Fig. 6(D) respectively. In addition to target protein biomarkers, a test sample also consists of range of different biomolecules and therefore there exists a probability for the capture probes to interact with these molecules and interfere in the detection of the target protein. This cross-reactivity for α-cTnI and α-cTnT was tested on multiplexed sensor arrays with BSA using varying concentrations diluted in HS in absence of protein biomarkers. BSA was chosen, as albumin is the main protein in human blood plasma. The measured EIS response is shown in Fig. 5(C-D) and measured Mott-Schottky capacitance response is shown in Fig. 6(C-D) respectively. The maximum percentage change in impedance observed with BSA using EIS was 5.8 % and 5.5 % respectively with α-cTnI and α-cTnT immobilized ZnO nanostructured sensing surfaces and is well within the established signal noise threshold. However, the maximum percentage change in capacitance observed with BSA using Mott-Schottky was 10 % and 7 % respectively with α-cTnI and α-cTnT immobilized ZnO nanostructured sensing surfaces. Although Mott-Schottky for BSA shows relatively high signal response it is still within the established signal noise threshold. Thus, the multiplexed sensor array with ZnO nanostructures showed good specificity and satisfying level of cross-reactivity for target cardiac biomarker and demonstrates the feasibility of detection in complex biological medium with both EIS and Mott-Schottky techniques.

4. Conclusions

In summary, we have developed a flexible and disposable semiconducting oxide nanostructure array based nanobiosensor platform that uses complementary electrochemical detection techniques i.e. EIS and Mott-Schottky for simultaneous and multiplexed detection of a panel of cardiac biomarkers i.e. cTnI and cTnT in human serum. The nanobiosensor platform comprises of a flexible polyimide substrate with zinc oxide nanostructures selectively grown on to the working electrode using hydrothermal growth methods. The growth conditions were optimized to ensure radial diffusion of the electrolyte i.e. human serum around the nanostructures. Sensitivity and selectivity in detection of these isoforms were demonstrated in a simultaneous manner with limit of detection at 1 pg/mL. Sensitivity and selectivity was achieved through measurement of capacitance modulations to the space charge region within the ZnO nanostructured electrode and also within the electrical double layer along the human serum electrolyte and ZnO nanostructured interface. Selectivity was established through cross-reactivity studies with the alternate isoform i.e. cTnI on a-cTnT treated array and cTnT on a-cTnI treated array as well as with bovine serum albumin. The capacitance changes to the space charge and electrical double layer were well within the noise threshold for the sensor array. Thus, we report for the first time multiplexed and simultaneous detection of cTnI and cTnT using multi-configurable

methods of EIS and Mott-Schottky capacitances. This multiplexed, simultaneous, and multi-configurable detection strategy using affinity based sensing as demonstrated on this nanobiosensor platform can be easily extended towards detection of other cardiac biomarkers and also for other disease based biomarkers and therefore promising in the design of next generation flexible point-of-care devices that have translation to clinical and portable diagnostics.

5. Acknowledgements

We would like to thank the Cecil and Ida A Green endowment in Systems Biology at the University of Texas, Dallas for supporting this research effort.

References

1. Agah, A., Hassibi, A., Plummer, J.D., Griffin, P.B., 2005. Design requirements for integrated biosensor arrays. Biomedical Optics 2005, pp. 403-413. International Society for Optics and Photonics.

2. Ahmad, M.I., Sharma, N., 2012. Biomarkers in acute myocardial infarction. Journal of Clinical & Experimental Cardiology 2012.

3. Apple, F.S., 2001. Cardiac troponin assays. Cardiovascular toxicology 1(2), 93-98.

4. Apple, F.S., Parvin, C.A., Buechler, K.F., Christenson, R.H., Wu, A.H., Jaffe, A.S., 2005. Validation of the 99th percentile cutoff independent of assay imprecision (CV) for cardiac troponin monitoring for ruling out myocardial infarction. Clinical Chemistry 51(11), 2198-2200.

5. Balasubramanian, K., 2010. Challenges in the use of 1D nanostructures for on-chip biosensing and diagnostics: A review. Biosensors and Bioelectronics 26(4), 1195-1204.

6. Bard, A.J., Abruña, H.D., Chidsey, C.E., Faulkner, L.R., Feldberg, S.W., Itaya, K., Majda, M., Melroy, O., Murray, R.W., 1993. The electrode/electrolyte interface-A status report. The Journal of Physical Chemistry 97(28), 7147-7173.

7. Daniels, J.S., Pourmand, N., 2007. Label‐free impedance biosensors: Opportunities and challenges. Electroanalysis 19(12), 1239-1257.

8. Feigel, I.M., Vedala, H., Star, A., 2011. Biosensors based on one-dimensional nanostructures. Journal of Materials Chemistry 21(25), 8940-8954.

9. Hewlett, R.M., McLachlan, M.A., 2016. Surface Structure Modification of ZnO and the Impact on Electronic Properties. Advanced Materials 28(20), 3893-3921.

10. Jaffe, A.S., Babuin, L., Apple, F.S., 2006. Biomarkers in acute cardiac disease: the present and the future. Journal of the American College of Cardiology 48(1), 1-11.

11. Joos, T.O., Stoll, D., Templin, M.F., 2002. Miniaturised multiplexed immunoassays. Current opinion in chemical biology 6(1), 76-80.

12. Koval, C.A., Howard, J.N., 1992. Electron transfer at semiconductor electrode-liquid electrolyte interfaces. Chemical reviews 92(3), 411-433.

13. Lei, Y., Luo, N., Yan, X., Zhao, Y., Zhang, G., Zhang, Y., 2012. A highly sensitive electrochemical biosensor based on zinc oxide nanotetrapods for L-lactic acid detection. Nanoscale 4(11), 3438-3443.

14. Liu, X., Lin, P., Yan, X., Kang, Z., Zhao, Y., Lei, Y., Li, C., Du, H., Zhang, Y., 2013. Enzyme-coated single ZnO nanowire FET biosensor for detection of uric acid. Sensors and Actuators B: Chemical 176, 22-27.

15. Marie, M., Mandal, S., Manasreh, O., 2015. An Electrochemical Glucose Sensor Based on Zinc Oxide Nanorods. Sensors 15(8), 18714-18723.

16. McDonnell, B., Hearty, S., Leonard, P., O'Kennedy, R., 2009. Cardiac biomarkers and the case for point-of-care testing. Clinical biochemistry 42(7), 549-561.

17. Morrison, S.R., 1980. Electrochemistry at semiconductor and oxidized metal electrodes.

18. Neumann, S., 2015. Biomarkers–Past and Future. Biomarker Validation, Technological, Clinical and Commercial Aspects, 1-22.

19. North, S.H., Lock, E.H., Taitt, C.R., Walton, S.G., 2010. Critical aspects of biointerface design and their impact on biosensor development. Analytical and bioanalytical chemistry 397(3), 925-933.

20. Qureshi, A., Gurbuz, Y., Niazi, J.H., 2012. Biosensors for cardiac biomarkers detection: a review. Sensors and Actuators B: Chemical 171, 62-76.

21. Shanmugam, N.R., Muthukumar, S., Selvam, A.P., Prasad, S., 2016. Electrochemical nanostructured ZnO biosensor for ultrasensitive detection of cardiac troponin-T. Nanomedicine 11(11), 1345-1358.

22. Thygesen, K., Alpert, J.S., Jaffe, A.S., White, H.D., Simoons, M.L., Chaitman, B.R., Katus, H.A., Apple, F.S., Lindahl, B., Morrow, D.A., 2012. Third universal definition of myocardial infarction. Journal of the American College of Cardiology 60(16), 1581-1598.

23. Wang, J., Sun, X.W., Wei, A., Lei, Y., Cai, X., Li, C.M., Dong, Z.L., 2006. Zinc oxide nanocomb biosensor for glucose detection. Applied physics letters 88(23), 233106-233106-233103.

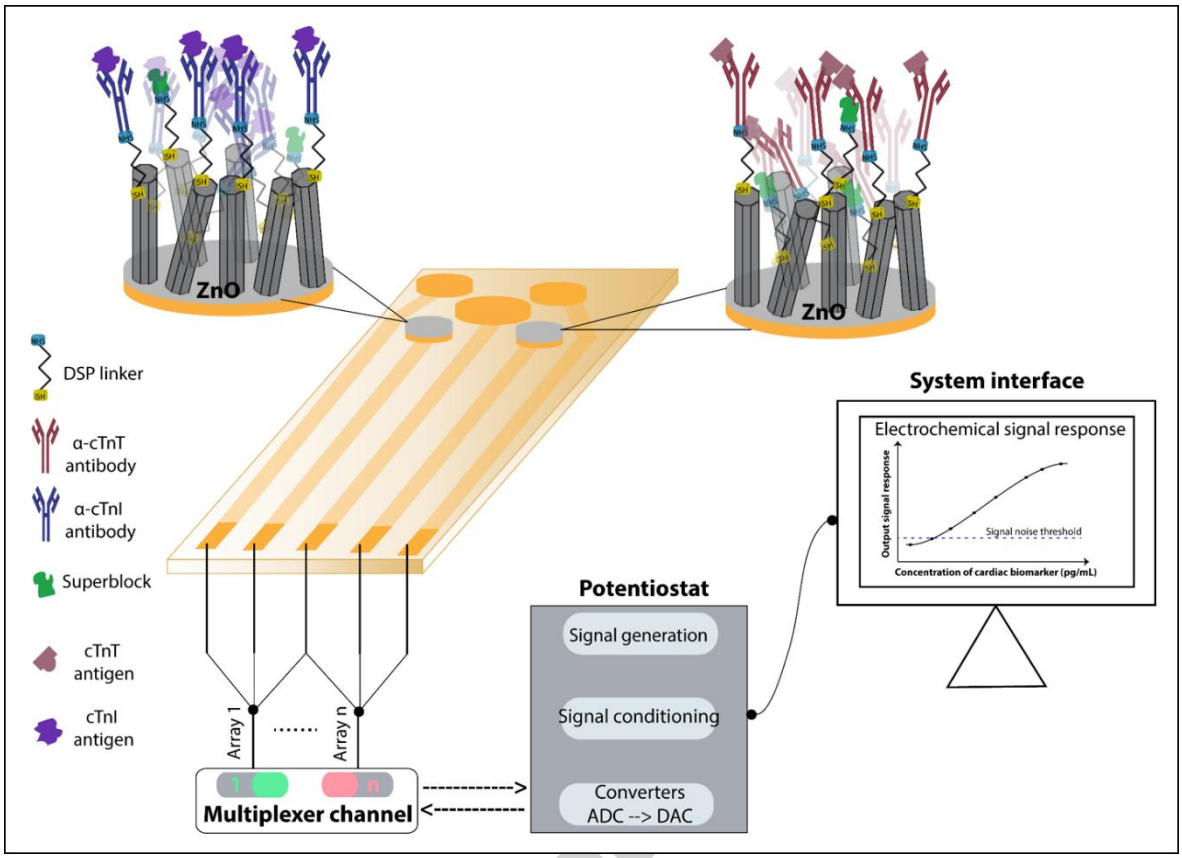

Figure 1. Schematic representation of sensing of cTnI and cTnT biomarkers in multiplexed sensor array format.

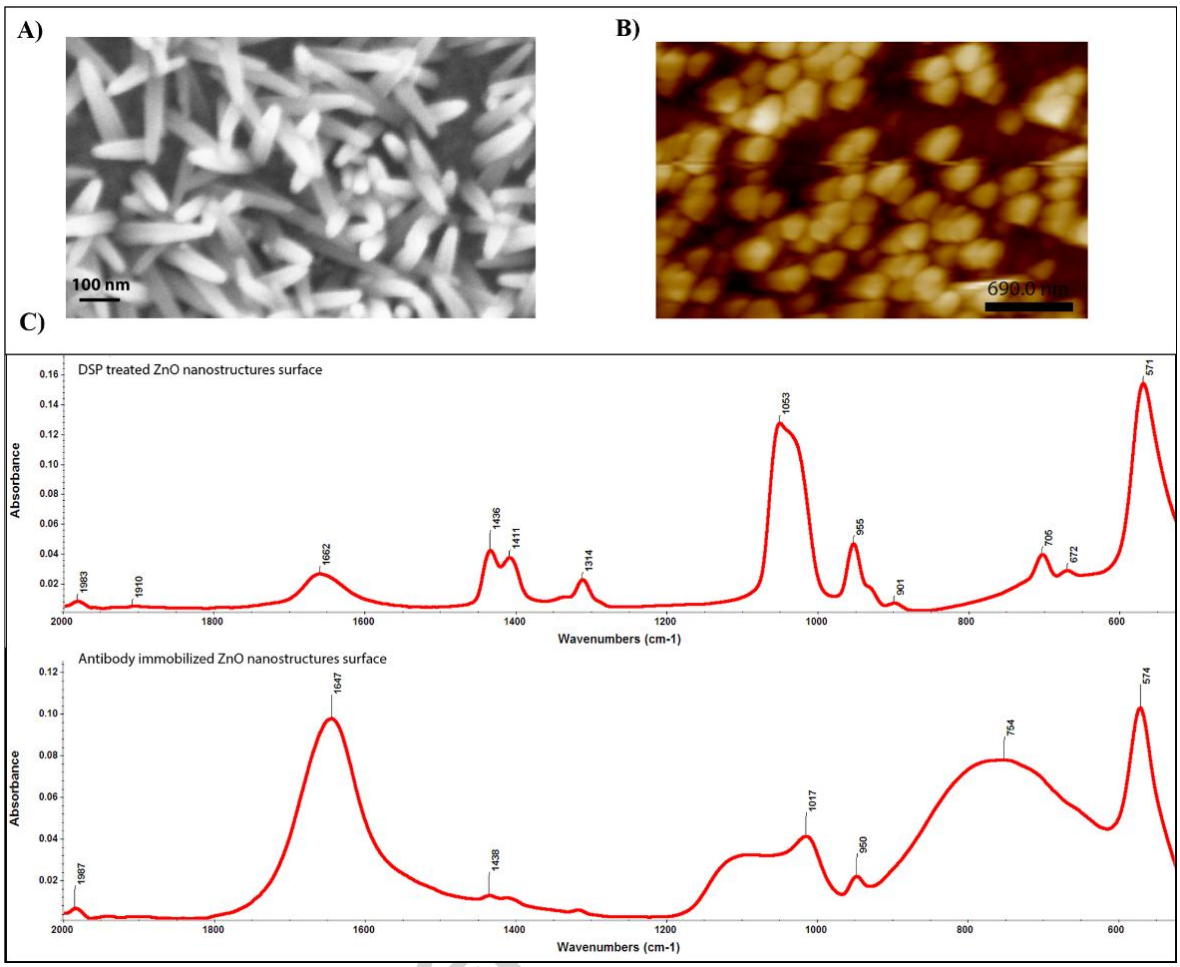

Figure 2. (A) SEM micrograph of ZnO nanostructures selectively grown at the working electrodes using hydrothermal growth mechanism. (B) AFM scan of ZnO nanostructures growth and (C) ATR-FTIR spectra showing the evidence of DSP functionalization (top) and antibody immobilization (bottom) on nanostructured ZnO sensing surface.

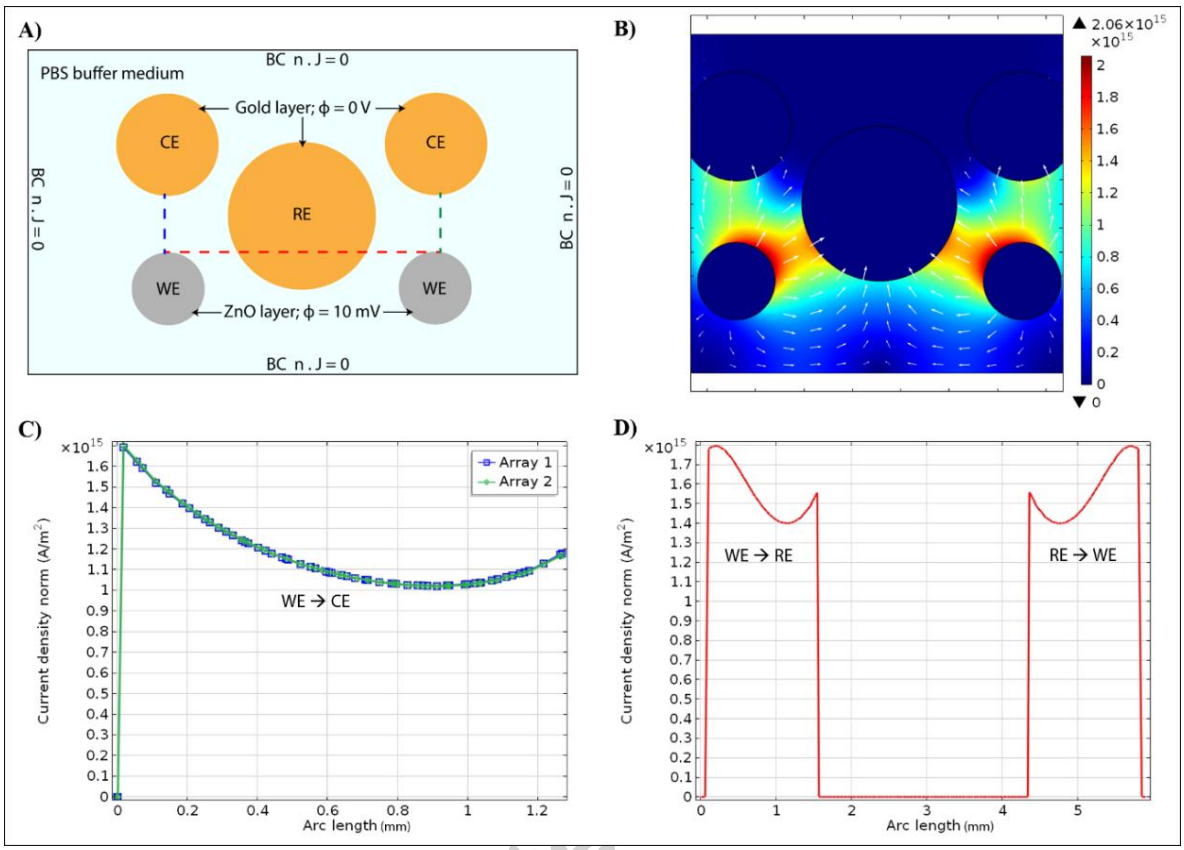

Figure 3. (A) Illustration of simulation geometry with applied boundary conditions. (B) Surface plot showing the distribution of current density and arrow plot representing the electric field distribution and its direction. (C) and (D) Line graph representing the current density distribution between the electrodes along the dotted lines as shown in (A). The dotted lines are colour coded as in graphical representations.

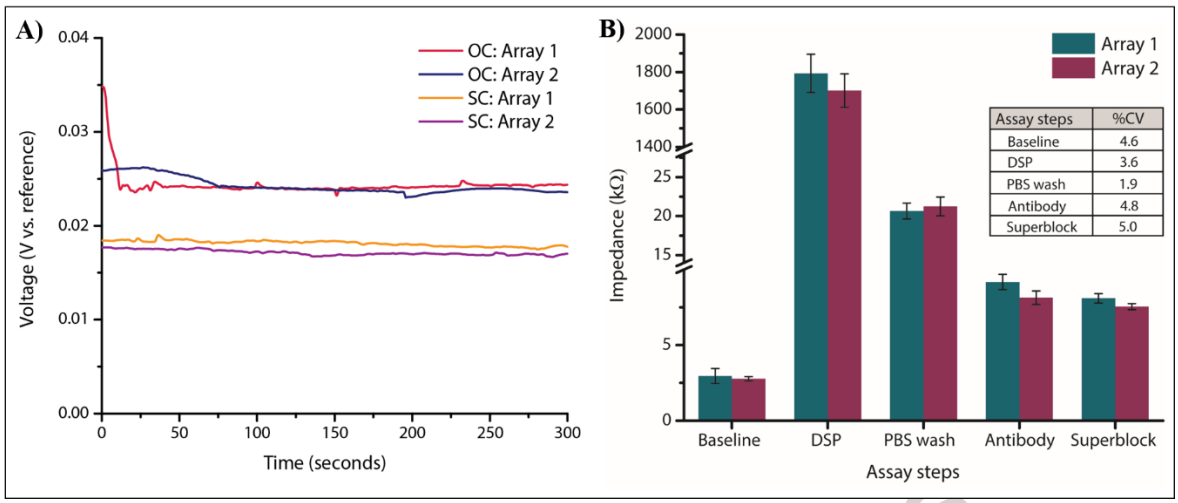

Figure 4. (A) Open-circuit and short-circuit potential measurements for array 1 and array 2 of the multiplexed ZnO sensor. The potential measured across both the arrays show the same trend with slight variation. (B) Baseline impedance characterization for various steps of immunoassay in both array 1 and array 2. Inset table gives the %CV in assay steps between array 1 and array 2. Data shown is from n=3 replicates.

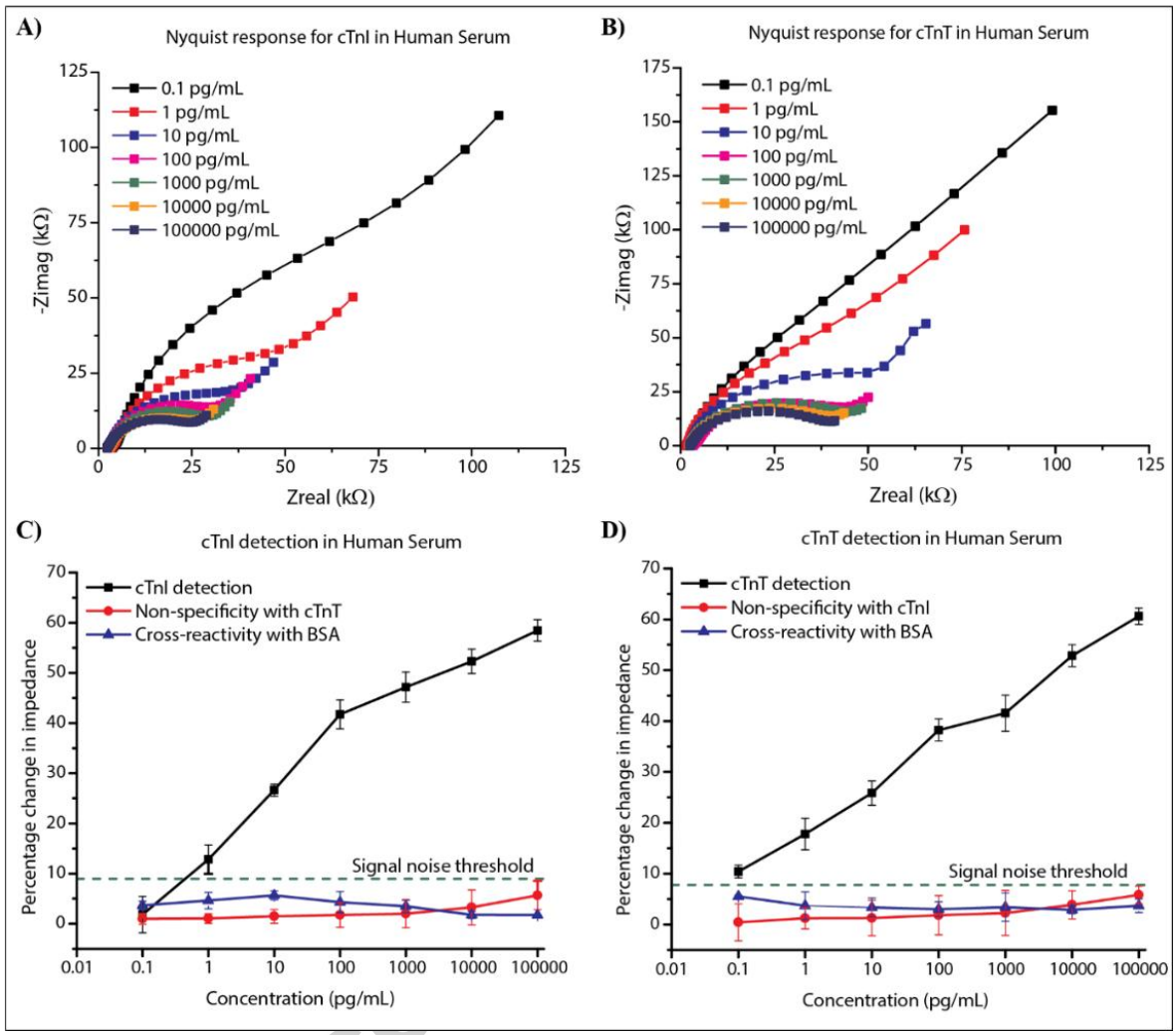

Figure 5. Multiplexed detection of cTnT and cTnI isoforms of cardiac biomarker using EIS technique. Nyquist plot for (A) cTnI antigen concentrations and (B) cTnT antigen concentrations showing decrease in impedance measurement with concentration indicating binding activity. Calibration dose response curve for simultaneous (C) cTnI detection and (D) cTnT detection in human serum. Control experimental results are also shown. Data is obtained from n=3 replicates and error bars represent 3SD from these replicates.

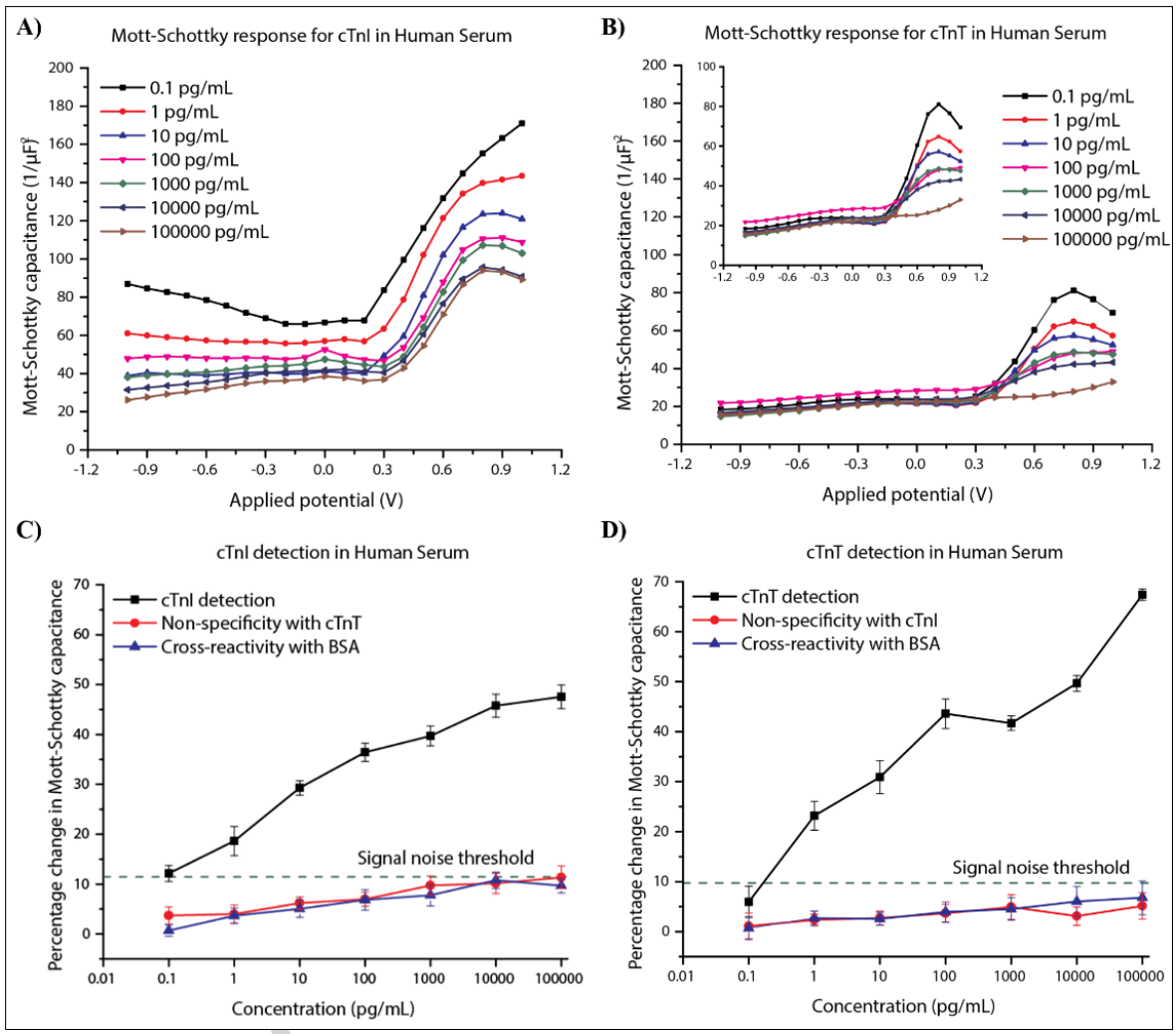

Figure 6. Multiplexed detection of cTnT and cTnI isoforms of cardiac biomarker using Mott-Schottky technique. Mott-Schottky capacitance plot for (A) cTnI antigen concentrations and (B) cTnT antigen concentrations indicating dose dependent change in measured signal output. Calibration dose response curve for simultaneous (C) cTnI detection and (D) cTnT detection in human serum. Control experimental results are also shown. Data is obtained from n=3 replicates and error bars represent 3SD from these replicates.

Research highlights

- Flexible zinc oxide nanostructured biosensors for multiplexed protein detection
- Multiplexed and simultaneous detection of two isoforms of troponins specific to acute myocardial infarction is demonstrated.
- Detection sensitivity and specificity is achieved through Electrochemical Impedance Spectroscopy and Mott Schottky analysis
- Quantitative detection established through simultaneous modulating space charge layer and electrical double layer.
- Limit of detection was established at 1 pg/mL in complex media; i.e. human serum.